

# PROCEEDINGS OF SPIE

[SPIDigitalLibrary.org/conference-proceedings-of-spie](https://spiedigitallibrary.org/conference-proceedings-of-spie)

## Deployment of the Hobby-Eberly Telescope wide field upgrade

Hill, Gary, Drory, Niv, Good, John, Lee, Hanshin, Vattiat, Brian, et al.

Gary J. Hill, Niv Drory, John Good, Hanshin Lee, Brian Vattiat, Herman Kriel, Randy Bryant, Linda Elliot, Martin Landriau, Ron Leck, David Perry, Jason Ramsey, Richard Savage, Richard D. Allen, George Damm, D. L. DePoy, Jim Fowler, Karl Gebhardt, Marco Haeuser, Phillip MacQueen, J. L. Marshall, Jerry Martin, Travis Prochaska, Lawrence W. Ramsey, Jean-Philippe Rheault, Matthew Shetrone, Emily Schroeder Mrozinski, Sarah E. Tuttle, Mark E. Cornell, John Booth, Walter Moreira, "Deployment of the Hobby-Eberly Telescope wide field upgrade," Proc. SPIE 9145, Ground-based and Airborne Telescopes V, 914506 (22 July 2014); doi: 10.1117/12.2057032

**SPIE.**

Event: SPIE Astronomical Telescopes + Instrumentation, 2014, Montréal, Quebec, Canada

# Deployment of the Hobby-Eberly Telescope Wide Field Upgrade<sup>†</sup>

Gary J. Hill<sup>a,‡</sup>, Niv Drory<sup>a</sup>, John Good<sup>a</sup>, Hanshin Lee<sup>a</sup>, Brian L. Vattiat<sup>a</sup>, Herman Kriel<sup>a,c</sup>, Randy Bryant<sup>c</sup>, Linda Elliot<sup>a</sup>, Martin Landtiau<sup>a</sup>, Ron Leck<sup>a</sup>, Dave Perry<sup>a</sup>, Jason Ramsey<sup>a</sup>, Richard Savage<sup>a</sup>, Richard D. Allen<sup>d</sup>, George Damm<sup>c</sup>, D.L. DePoy<sup>d</sup>, Jim Fowler<sup>c</sup>, Karl Gebhardt<sup>b</sup>, Marco Haeuser<sup>d</sup>, Phillip MacQueen<sup>a</sup>, J.L. Marshall<sup>d</sup>, Jerry Martin<sup>c</sup>, Travis Prochaska<sup>d</sup>, Lawrence W. Ramsey<sup>e</sup>, Jean-Philippe Rheault<sup>d</sup>, Matthew Shetrone<sup>c</sup>, Emily Schroeder Mrozinski<sup>c</sup>, Sarah E. Tuttle<sup>a</sup>, Mark E. Cornell<sup>g</sup>, John Booth<sup>a</sup>, Walter Moriera<sup>h</sup>

<sup>a</sup> McDonald Observatory, <sup>b</sup> Department of Astronomy, <sup>c</sup> Hobby-Eberly Telescope, University of Texas at Austin, 2515 Speedway, C1402, Austin, TX 78712, USA

<sup>d</sup> Department of Physics and Astronomy, Texas A&M University, 4242 TAMU, College Station, TX 77843, USA

<sup>e</sup> Universitäts-Sternwarte München, Scheinerstr. 1, 81679 München, Germany

<sup>f</sup> Department of Astronomy, Pennsylvania State University, 516 Davey Lab, University Park, PA 16802, USA

<sup>g</sup> MIT Lincoln Laboratory, ETS Field Site, P.O. Box 1707, Socorro, NM 87801, USA

<sup>h</sup> Texas Advanced Computing Center, University of Texas at Austin, Research Office Complex 1.101, J.J. Pickle Research Campus, Building 196, 10100 Burnet Road, Austin, Texas 78758, USA

## ABSTRACT

The Hobby-Eberly Telescope (HET) is an innovative large telescope located in West Texas at the McDonald Observatory. The HET operates with a fixed segmented primary and has a tracker, which moves the four-mirror optical corrector and prime focus instrument package to track the sidereal and non-sidereal motions of objects. A major upgrade of the HET is in progress that will substantially increase the pupil size to 10 meters (from 9.2 m) and the field of view to 22 arcminutes (from 4 arcminutes) by replacing the corrector, tracker, and prime focus instrument package. In addition to supporting existing instruments, and a new low resolution spectrograph, this wide field upgrade will feed a revolutionary new integral field spectrograph called VIRUS, in support of the Hobby-Eberly Telescope Dark Energy Experiment (HETDEX<sup>§</sup>). The upgrade is being installed and this paper discusses the current status.

**Keywords:** Telescopes: Hobby-Eberly, HET, HETDEX, wide field corrector, tracker, spectrographs: VIRUS

## 1. INTRODUCTION

The HET<sup>1-6</sup> (Fig. 1) is an innovative telescope designed to be cost-effective for large surveys. It has an 11 m hexagonal-shaped spherical primary mirror made of 91 1-m hexagonal segments that sits at a fixed zenith angle of 35°. HET is the basis for the Southern African Large Telescope (SALT)<sup>7</sup>. It can be moved in azimuth to access about 70% of the sky visible at McDonald Observatory ( $\delta = -10.3^\circ$  to  $+71.6^\circ$ ). The pupil is 9.2 m in diameter, and sweeps over the primary mirror as the x-y tracker follows objects for between 50 minutes (in the south at  $\delta = -10.0^\circ$ ) and 2.8 hours (in the north at  $\delta = +67.2^\circ$ ). The maximum time on target per night is 5 hours and occurs at  $+63^\circ$ . The HET primary mirror has a radius of curvature of 26164 mm, and the current 4-mirror double-Gregorian type corrector is designed to produce images with FWHM  $< 0.6$  arcsec in the absence of seeing, over a 4 arcmin (50 mm) diameter science field of view. Detailed descriptions of the original HET and its commissioning can be found in refs 1-6.

<sup>†</sup> The Hobby – Eberly Telescope is operated by McDonald Observatory on behalf of the University of Texas at Austin, Pennsylvania State University, Ludwig-Maximilians-Universität München, and Georg-August-Universität, Göttingen

<sup>‡</sup> G.J.H.: E-mail: hill@astro.as.utexas.edu

<sup>§</sup> <http://hetdex.org/>

The HET was envisioned originally as a spectroscopic survey telescope, able to efficiently survey objects over wide areas of sky. While the telescope has been very successful at observing large samples of objects such as QSOs and extrasolar planets spread over the sky with surface densities of around one per 10 sq. degrees, the HET design coupled with the limited field of view of the original corrector hampers programs where objects have higher sky densities. In seeking a strong niche for the HET going forward, the HET field of view will be increased from  $4^\circ$  to  $22^\circ$  so that it can accommodate the Visible Integral-field Replicable Unit Spectrograph (VIRUS)<sup>8-11</sup>, an innovative, highly multiplexed spectrograph that will place 35,000 fibers on sky simultaneously and open up the emission-line universe to systematic surveys for the first time, uncovering populations of objects selected by their line emission rather than by their continuum emission properties.

The primary motivation for the HET wide field upgrade (WFU) and VIRUS is to execute the Hobby-Eberly Telescope Dark Energy Experiment (HETDEX<sup>12</sup>), which will map the spatial distribution of about 0.8 million Ly $\alpha$  emitting galaxies (LAEs) with redshifts  $1.9 < z < 3.5$  over a 420 sq. deg. area ( $9 \text{ Gpc}^3$ ) in the north Galactic cap. This dataset will constrain the expansion history of the Universe to 1% and provide significant constraints on the evolution of dark energy. The requirement to survey large areas of sky with VIRUS plus the need to acquire wavefront sensing stars to provide full feedback on the tracker position led us to design an ambitious new corrector employing meter-scale aspheric mirrors and covering a 22-arcmin diameter field of view.

The WFU deploys the wide field corrector (WFC<sup>13,14</sup>), a new tracker<sup>15,16</sup>, a new prime focus instrument package (PFIP<sup>17,18</sup>), and new metrology systems<sup>17-23</sup>. The metrology systems are intended to provide closed-loop feedback on all axes of motion and the optical configuration of the telescope. They include guiding, wavefront sensing, payload tilt sensing, and a distance measuring interferometer (DMI). Together they control the alignment of the WFC to the primary mirror as well as providing feedback on the temperature-dependent radius of curvature of the primary mirror, which is on a steel truss.

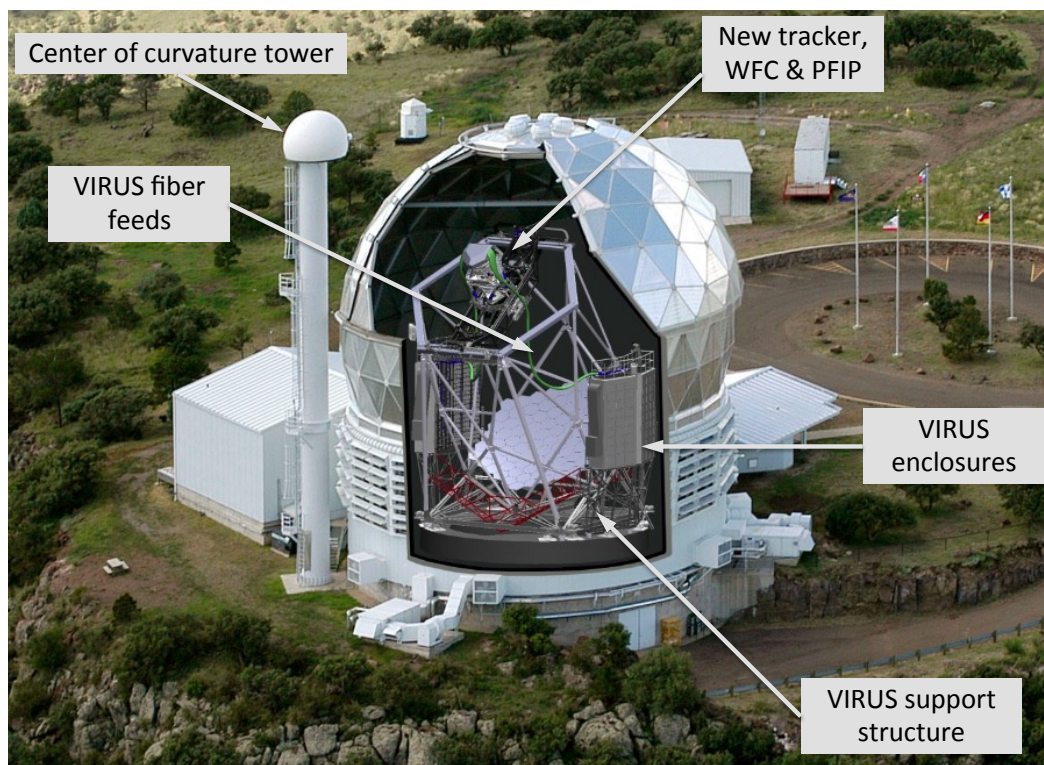


Figure 1. The layout of the HET with rendering of the WFU and VIRUS superimposed. The WFU replaces the top end of the HET with a new tracker, wide field corrector (WFC) and prime focus instrument package (PFIP). The highly replicated VIRUS spectrograph units are housed in two enclosures either side of the structure, which are mounted on the VIRUS support structure, and fed by 33,000 fibers from the prime focus.

## 2. TELESCOPE CONFIGURATION

The basic configuration of the HET is unchanged in the upgrade, but the new tracker has a much higher payload of 3 tonnes to accommodate the new WFC and PFIP. VIRUS is fiber-fed which allows the mass of the spectrographs to be carried in two enclosures one on each side of the telescope (Fig. 1). Each enclosure can support 40 pairs of spectrographs (VIRUS units have two spectrograph channels, and disperse the light from an IFU with 448 fibers), there is capacity for a total of 80 units. The likely deployed size of VIRUS will be between 75 and 78 units (up to 156 spectrographs with coverage per observation of over 60 sq. arcminutes. Figures 1 and 2 show CAD renderings of the telescope post upgrade and identify the major components.

The key configuration change to the facility is the addition of the enclosures and support structure for VIRUS (Figure 1). The location of the spectrograph enclosures was constrained by many factors, including:

- " Desire to maximize throughput (especially in the UV) by minimizing the length of the fiber feeds
- " Minimize the mechanical stress on the fiber feeds
- " Maintain adequate man-lift access to the telescope's interior structure. This is particularly important because the mirror segments are cleaned with CO<sub>2</sub> several times a week, and the individual mirror segments are removed and recoated on a regular basis.
- " Prevent wind-induced motion of the spectrograph enclosures (which have an effective wind sail area on the order of 50 m<sup>2</sup>) from shaking the telescope structure and causing image degradation
- " Minimize complexity, weight, and cost of the structure, which supports the spectrograph enclosures

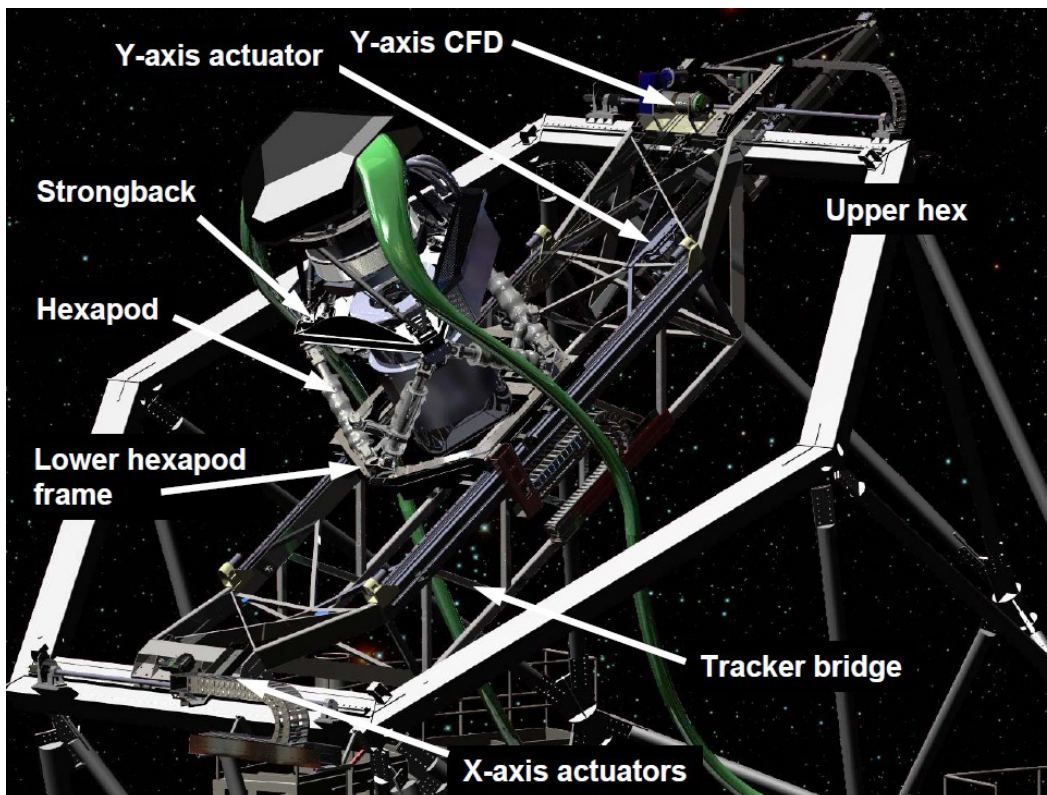


Figure 2. Close up view of the top of the telescope post WFU with key components indicated. New features compared to the old HET tracker are the center drive on the y-axis and the addition of the y-axis constant force drive (CFD).

The final enclosure locations were a compromise that was strongly influenced by the need to maintain man lift access to the primary mirror. The VIRUS Support Structure<sup>24</sup> is a complex weldment that interleaves with the main telescope structure without applying loads to it that could couple wind induced vibration from the enclosures to the telescope. It rides on separate air-bearings that lift it during changes in telescope azimuth, and is pulled round by the main azimuth

drive. The enclosures are large clean rooms with air circulation and heat extraction to remove heat from the VIRUS controllers and ensure that the skin temperature of the enclosures remains close to ambient to ensure they do not impact the dome seeing.

### 3. TRACKER

A new tracker is needed to accommodate the size and five-fold weight increase of the new WFC and PFIP. It represents a third generation evolution of the trackers for HET and SALT, and is in essence a precision six-axis stage (Figs. 3, 4). The tracker bridge spans the upper hexagon of the telescope structure, moving on two x-axis stages with skew sensing in case they become misaligned. A carriage moves up and down in the y-axis, and supports the hexapod that provides the fine adjustment in the other degrees of freedom. The total volume of motion is about  $7 \times 7 \times 4 \text{ m}^3$ , and the required accuracy is on the order of  $10 \text{ }\mu\text{m}$  and 4 arcseconds in tilt.

The tracker was built by the Center for Electro-Mechanics (CEM) and McDonald Observatory (MDO) at the University of Texas at Austin<sup>25-28</sup>. After integration and testing was finished it underwent a test plan that was completed in mid 2013<sup>16</sup>. Testing was based on using a laser tracker (LT, model API T3-40 with DMI) to map out deflections in six degrees of freedom relative to an ideal spherical surface, surrogate for the HET primary mirror focal surface. The accuracy of the measurements was below 100 microns, well within the capture range of metrology systems to be deployed with the upgrade. We demonstrated that the deviations from a sphere were well-behaved and had residuals better than 100 microns, and that we could adjust the working point of the track axially. The latter is required to match the tracking sphere to the point where the WFC can be tilted without moving the image (the stationary-image rotation point or SIRP). We further verified that guide offsets could be executed within the required time and to better than the required accuracy. The performance testing is described in Ref. 16. Following a Readiness Review in July 2013 for the upgrade, the new tracker was packed and shipped in stages as the old HET tracker was dismantled and the structure prepared for the installation of the new tracker by welding on stiffening sections on the upper and lower beams of the top-hexagon. The upper and lower X-axes were installed in late 2013. The tracker bridge was the last major item to be shipped and installed over 2 days in February 2014 with a large external crane. As of the time of writing the tracker is functional and able to execute moves and tracks, and we are starting testing and mount modeling. Figure 3 shows the current state of the tracker, installed on HET and details of the tracker installation and commissioning status can be found in Ref 16.

The tracker is a precision machine that was subject to numerous challenging design constraints, including the following:

- " Accurately positioning the WFC/PFIP during observations to maintain image quality. The design goal is to maintain the position and orientation of the WFC with respect to the primary mirror to within a decenter of  $10 \mu\text{m}$ , a defocus of  $10 \mu\text{m}$ , and tip/tilt to within 4#.
- " Minimizing tracker obstruction of the primary mirror with a bridge structure optimized with finite element analysis.
- " Reducing the overall weight of the tracker to keep it within the load bearing capacity of the existing telescope structure, and to achieve a fundamental mode of the entire telescope above 5 Hz.
- " Accommodating the limited overhead dome crane lifting capacity and hook height, which constrained the maximum weight and geometry of the tracker carriage, hexapod, and PFIP components. These constraints precluded the possibility of assembling the entire carriage/hexapod/PFIP assembly on the ground and then lifting it to the top of the telescope as a single assembly. Instead, several smaller assemblies must be lifted to the top of the telescope (one at a time) and then assembled at height over the primary mirror, a precarious process which subjects the primary mirror to increased risk of damage.
- " Preventing the tracker carriage/hexapod/PFIP assembly from ever experiencing a down-hill free-fall along the tracker Y axis. Such an accidental event could result in catastrophic damage to the telescope. CEM conducted a thorough failure mode and effects analysis (FMEA<sup>29</sup>) which resulted in a redundant design solution that has multiple layers of failure prevention. This includes the design of constant force actuator safety system<sup>25</sup> which is similar to the one used on the Southern African Large Telescope.
- " Preventing a tracker hexapod actuator failure from damaging the PFIP/WFC. This required a thorough understanding of the volume swept out by the PFIP/WFC for all plausible combinations of the hexapod actuator lengths<sup>26</sup>.
- " Accommodating the limited straightness, flatness, and flexure of the tracker x-axis and y-axis linear bearing rail mounting surfaces, and long linear axis travel ranges (especially with regards to lead screw sag and critical speed).

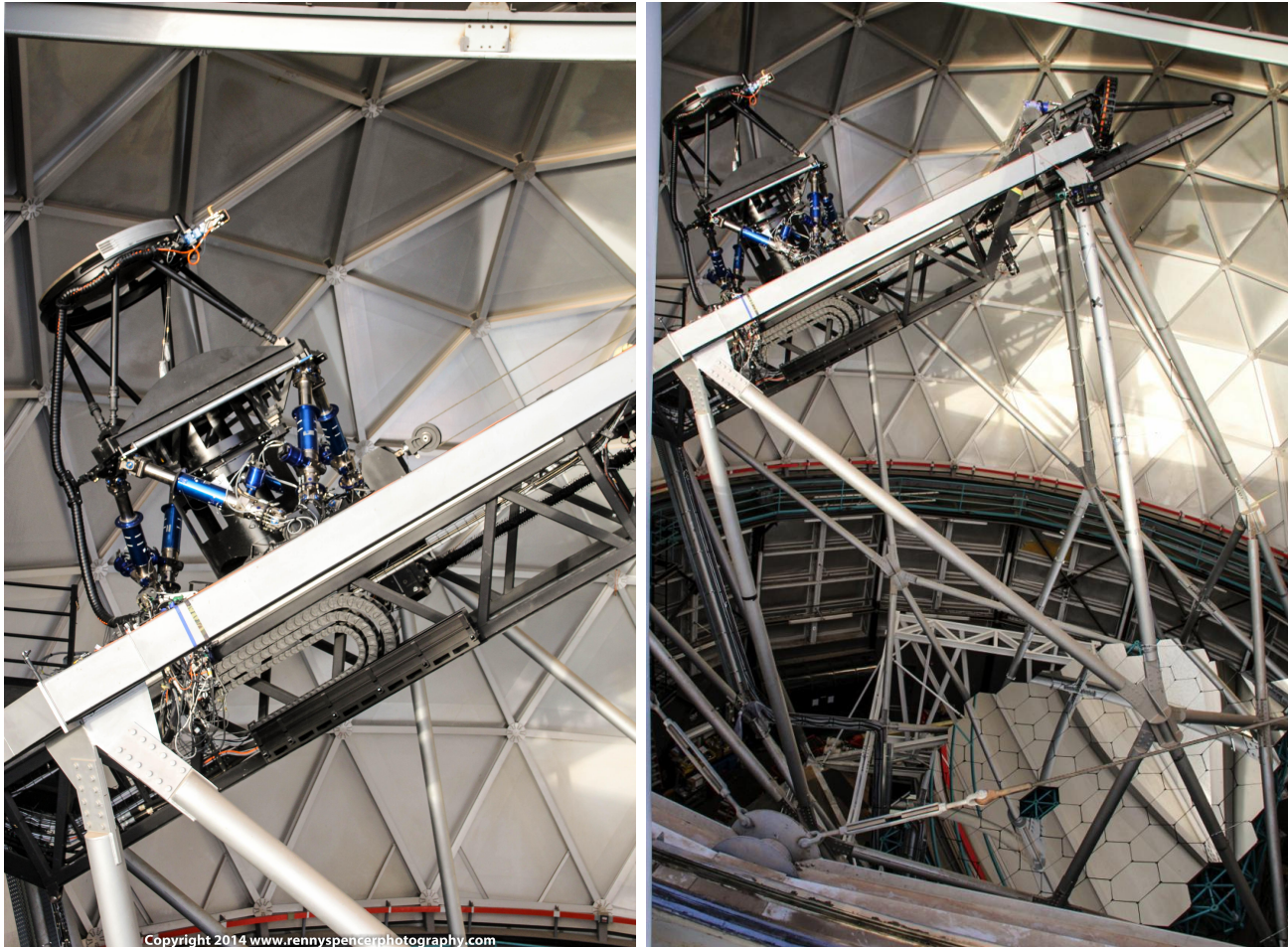


Figure 3. Assembled and functional tracker on HET. The hexapod struts can be identified by their blue casings.

Differences between the new tracker and the previous HET tracker include the provision of a center drive on the y-axis (rather than a side drive screw) and the addition of a constant-force drive winch system as a safety measure on the y-axis. Both changes were necessitated by the significantly higher moving mass and analysis that showed unacceptable forces generated by impact of the tracker payload should there be a run-away in the y-axis, down-hill. The constant force drive uses an independent drive system with load-cell feedback to un-weight part of the load, but its primary purpose is to sense a runaway condition and apply a brake that is independent of the rest of the control system. This scheme provides safety for both equipment and personnel, and was settled upon following a detailed failure modes and effects analysis.

The hexapod actuators were manufactured by ADS International (Valmadrera, Italy) in collaboration with CEM and MDO<sup>26</sup>. A hydraulic test bed for the struts was built at CEM to test them in compression and tension over their operating range and to map residual errors in position versus encoder values. The actuator shaft rotations are encoded. The LT was used for this “mount-model” which exhibited only very small deviations from linear. Assembly into the hexapod configuration was first done in a vertical orientation. Following tests and initial characterization the assembled hexapod was mounted at 35 degrees in its test stand to mimic the posture on HET. In this configuration the control system was tested and positions confirmed with the LT to verify algorithms. The hexapod was subsequently mounted on the Y carriage following testing of the x- and y-axes with a dummy test mass on the carriage.

The tracker motion control system (TMCS) is based in the Matlab-Simulink environment in a dSPACE controller<sup>27,30</sup>. The Telescope Control System (TCS) handles all the high-level functions and most of the coordinate transforms and mount models for the tracker. Limitations within the TMCS environment limit the ability to perform complex calculations on the 2.5 ms update rate, so TCS interprets all the higher-level functions for the TMCS and receives status updates 5 times per second through the API. Development of the TMCS at CEM lagged significantly and necessitated MDO personnel taking over responsibility for the system. While the tracker was dismantled and being installed we built a software model for the tracker to enable further development of the TMCS and the TCS in concert. This proved invaluable, since several architecture issues with the TMCS were not uncovered and fixed until this phase. At the time of writing, the TCS-TMCS is able to command the tracker from the GUI level and execute moves and tracks as needed for commissioning.

#### 4. WIDE FIELD CORRECTOR

The new corrector (Fig. 4) has improved image quality over a 22 arcminute diameter field of view and a 10 m pupil diameter. The periphery of the field will be used for guiding and wavefront sensing to provide the necessary feedback to keep the telescope correctly aligned. The WFC is a four-mirror design with two concave 1 meter diameter mirrors, one concave 0.9 meter diameter mirror, and one convex 0.23 m diameter mirror. The corrector is designed for feeding optical fibers at  $f/3.65$  to minimize focal ratio degradation, and so the chief ray from all field angles is normal to the focal surface. This is achieved with a concave spherical focal surface centered on the exit pupil. The primary mirror spherical aberration and the off-axis aberrations in the wide field are controllable due to the first two mirrors being near pupils, and the second two mirrors being well separated from pupils to control field aberrations. The imaging performance is 0.6 arcsec or better over the entire field of view, and vignetting is minimal. The WFC is being manufactured by the University of Arizona College of Optical Sciences (OSC)<sup>13,14</sup>.

Figuring and polishing of the three large mirrors was done at OSC on robotic swing-arm machines and tested with swing-arm profilometry using non-contact sensors (Fig. 5). The degree of aspheric departure and the steepness of the surfaces of the large mirrors proved a challenge. Testing of the large mirrors used a combination of non-contact swing-arm profilometry, tied to laser tracker measures of the radius of curvature, and Interferometric confirmation of figures using phase etched computer generated holograms (CGHs) is proceeding. Testing was completed in March 2013. As part of the figure test, centering fixtures were aligned that were intended to be used in the final alignment of the WFC assembly. These center fixtures have CGH targets that provide a reference that locates the center and normal of each mirror surface. The smaller M4 was subcontracted to Precision Asphere, and utilized a transmission test with CGH (Fig. 5).

Reflective coatings for the WFC are required to have high reflectance (95% or better from 350 nm 1800 nm), and are challenging, being based on silver and multiple dielectric layers. Experience with coating degradation on the old HET corrector led us to adopt a sealed design for the WFC with entrance and exit windows and careful sealing of the WFC housing. The WFC will be purged with nitrogen gas. The facility will have a large volume of nitrogen available from the cooling system for VIRUS, and this will be utilized to provide an over-pressurized oxidation-free environment for the mirror coatings to achieve the longest life possible. The large mirrors were coated by JDSU and M4 will be recoated in August by Zecoat following failure of the initial coating by a different vendor. M4 sees a very wide range of incident angles, and requires a more complex coating than the others. MDO designed and constructed the complex fixturing needed to safely support the large mirrors during cleaning and coating at JDSU<sup>31</sup>.

The structure of the WFC is a space frame, which is mounted kinematically into the PFIP and tracker (Fig. 4). FEA analysis focused on maintaining critical alignments between the mirrors as the corrector moves between the extreme angles of 25 to 45 degrees. In particular the separation of M4 and M5 has to be held to a few microns, and their very different masses make this a challenge. OSC designed tunable flexures for the M4 supports that allow the relative motion of these two mirrors to be tuned. MDO supplied test masses that mimic the mass and center of gravity<sup>31</sup> of the mirrors to allow testing of the structure and tuning of these flexures prior to completion of the mirrors. Tests with a laser tracker indicate all displacements are within specification and have allowed the tuning of the flexures to null out the relative motion of M4 and M5. The structure was thus qualified ahead of the completion of the mirrors.

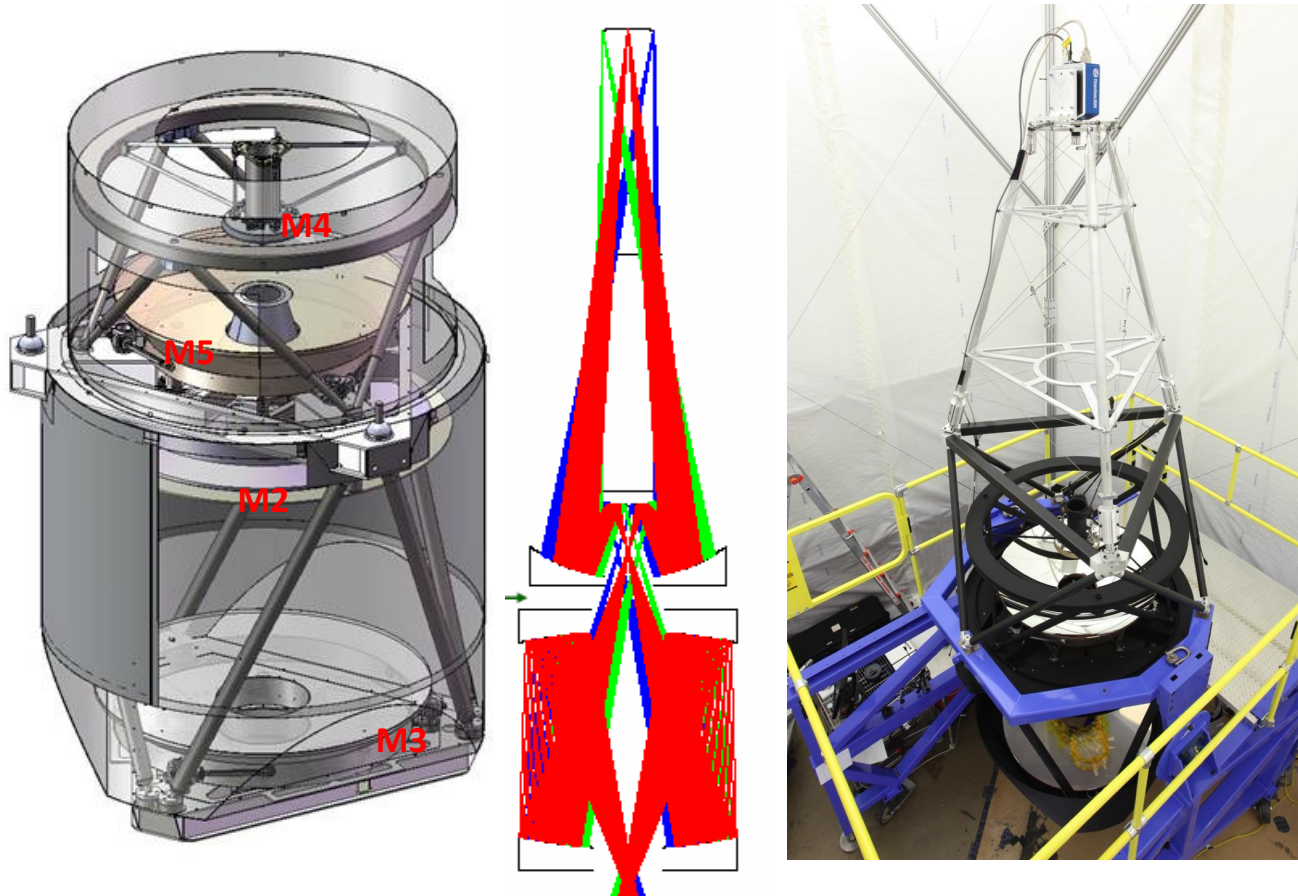


Figure 4. Layout of WFC mirrors and structure (left), and WFC structure undergoing tests with dummy mirrors to confirm performance and tune flexures for M4 supports (right).

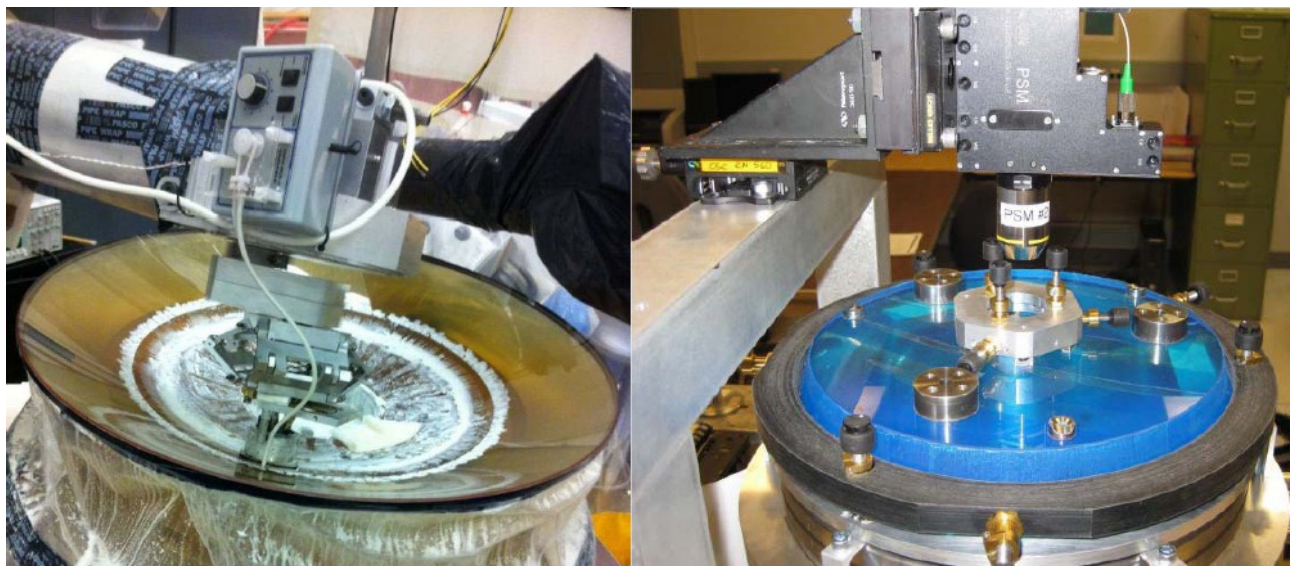


Figure 5. Polishing of M3 mirror on robotic machine at OSC (left), and M4 (convex aspheric) metrology setup for bonding and aligning center reference CGH (right).



The alignment scheme developed by UA OSC relied on the center references to locate the mirror surfaces using a combination of an interferometer and autocollimator to set centration and tilts and a LT to set separations. Then interferometric CGH tests of the M4/M5 pair the M2/3 pair and of the whole system were to be used to evaluate the alignment of the assembly. An independent conjugate test of the M4/5 pair with a custom wavefront sensor was developed by MDO staff to provide an independent confirmation that the system is meeting specification, particularly in off-axis performance. The system test will be repeated with the wavefront sensor before shipping and will be used to check alignment once the corrector is delivered to HET.

The alignment process was initiated in September 2013 following integration of the mirrors into the WFC structure. It was discovered that the center references had drifted in tilt due to the choice of silicone to bond the references following alignment. Following diagnosis of this problem, an alternative alignment scheme utilizing the M2/3 and M4/5 subsystem interferometric CGH pair tests was developed to align in tilt. The center references were sufficient for centration and separation. In February 2014 this scheme was started with the M4/5 pair. Inconsistency in the wavefront measured for this pair indicated an error on the figure of one of the mirrors, which was eventually traced to M5 having a significantly different figure than established in the original tests, due to errors in analysis<sup>14</sup>. Subsequent review revealed a significant error in M3 also. Following an extensive period of review and execution and analysis of the M4/5 CGH pair test, the M2/3 CGH pair test and the UT M4/5 conjugate test, we have achieved an understanding of the figures of each mirror within the required error bounds to meet specification.

The spacing of mirrors in the prescription of the WFC has been re-optimized by MDO in conjunction with an aspheric corrector plate and a separate configuration for the atmospheric dispersion corrector (ADC). The resulting prescription meets the original image quality requirements. OSC is proceeding to align the corrector, and MDO is procuring the aspheric corrector plate. The plate will be used for the system test that still provides the final gate for acceptance of the WFC. The schedule indicates the end of 2014 or early 2015 for completion, allowing some contingency.

Since the corrector should now be regarded as being a 5-element design, including the corrector plate, the system test must include the corrector plate. The reflective CGH in the system test essentially mimics the wavefront from the primary mirror, so the system test should provide confirmation of the final delivered wavefront, expected on-sky, on axis. We intend to perform on-sky tests with wavefront sensors deployed over the field of view (mounted in the VIRUS IFU seats in the input head mount plate, see below) as a final confirmation of the performance of the WFC prior to procuring the second corrector plate (coated for NIR wavelengths) and the ADC.

## 5. PRIME FOCUS INSTRUMENT PACKAGE

The PFIP<sup>17,18</sup> rides on the tracker and consists of several subassemblies. The Wide Field Corrector (WFC) mounts on a strongback on a three ball-in-vee kinematic mount. The strongback mounts to the tracker hexapod and the structure of PFIP is built up around the corrector. The focal plane assembly (FPA), shown in Fig. 6, contains all the hardware at the focus of the telescope including the acquisition and guiding (AG) assembly, fiber instrument feeds, shutter, and electronics hardware. The Lower Instrument Package (LIP) is mounted to the input end of the wide field corrector and is a platform for the entrance window changer, tip-tilt camera, and facility calibration unit (FCU) output head. A set of temperature controlled, insulated enclosures house electronics hardware and the FCU input sources, optics, and selection mechanisms. The pupil plane assembly (PPA) is located in between the wide field corrector and the focal plane assembly. It contains a stationary and moving set of baffles at the exit pupil of the telescope and a platform for selectable exit windows (now aspheric corrector plates) and the atmospheric dispersion compensator (ADC) for the wide field corrector. The deployment of the PPA is split into two phases. Initially, the support structure with fixed exit pupil baffle and the corrector plate is being deployed. Since the design of the PPA has to be updated to accommodate the tighter positioning requirements of the corrector plates (one each for optical and NIR bandpasses) the full system will be deployed after the HET is commissioned and the image quality performance is verified. The second corrector plate and ADC will be procured following confirmation of wavefronts with on-sky WFS measurements.

The heart of the metrology system for the WFU is the AG assembly (Fig 6 & 7), which mounts the guide probe assembly, the acquisition camera, a wavefront sensor and a pupil viewer. The light is directed to these by deployable pickoff mirrors with pneumatic actuators. The guide probe assembly is used for star guiding of the telescope and wavefront sensing feedback to the telescope focus. There are four probes; two imaging probes and two wave-front

sensing probes. Each probe consists of a probe optical head, containing the necessary optics coupled to a coherent fiber bundle purchased from Schott. Images incident to the fiber bundle input are captured by a remote camera system (FLI Proline) at the bundle output, fed by reimaging optics and including a filter wheel for each of the guide probes. Each probe optical head is mounted to a carriage with an arm for moving the probe radially in the field with a range of 9-11 arcminutes from the center of the telescope's field. The four carriages each move through 180° sectors on large bearings to access stars (Fig. 7). The positioning accuracy requirement of the guide probes is 20 microns on the spherical focal surface. To achieve this, both mechanical position actuation and encoding required a high level of precision. The acquisition camera has 3 arcminute field of view and can be used simultaneously with the GPs and WFS in the guide probe assembly.

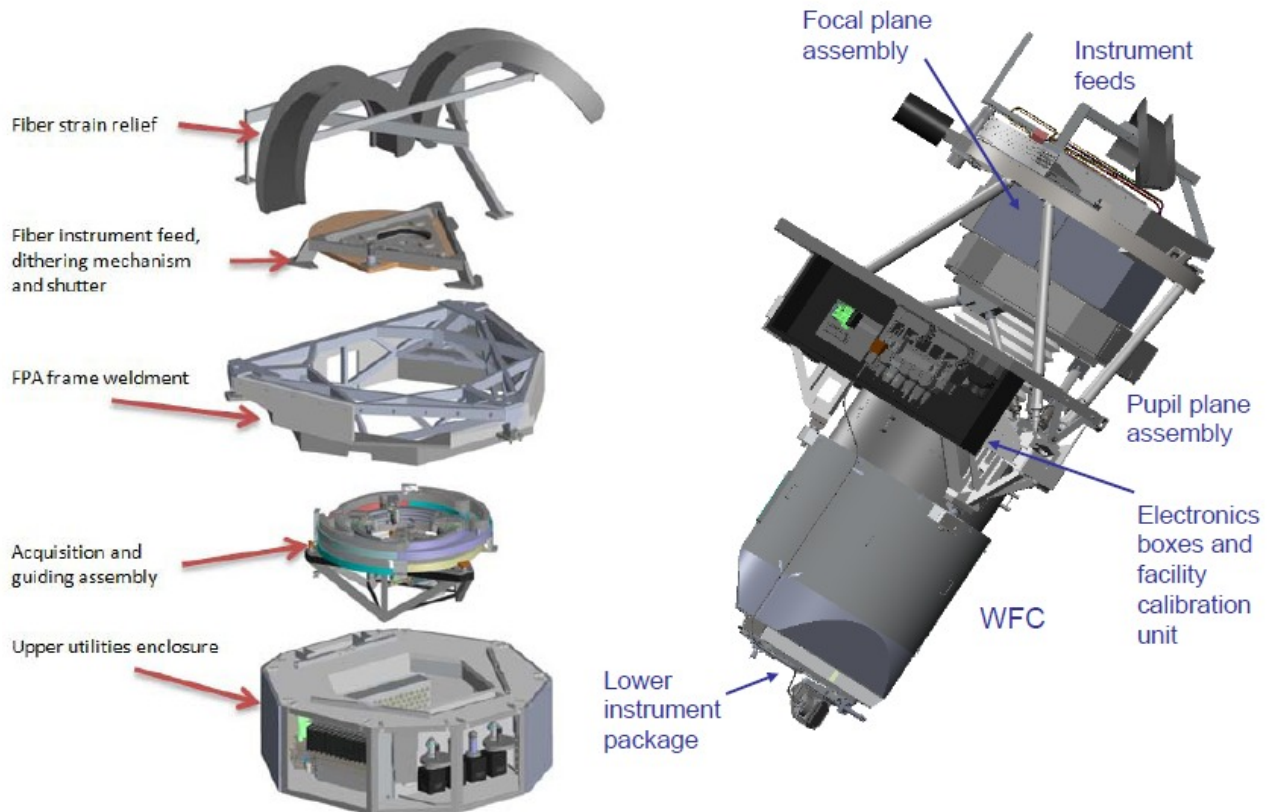


Figure 6. Renderings of the PFIP. On the right the full assembly is shown with major sub-assemblies indicated. On the left is an exploded view of the FPA showing its major components. The FPA contains most of the complexity of the instrument, including the acquisition and guiding (AG) assembly with guide probes and wavefront sensors.

The prime focus shutter, which shutters VIRUS and LRS2 is a rotary-type shutter initially inspired by the FORS shutter design. The shutter “blade” is a rotating disc with an aperture cut out of one section. Exposure occurs when the disc rotates so that the aperture aligns with the clear aperture of the focal surface. The shutter blade itself is a custom cut sheet of carbon fiber reinforced plastic (CFRP) purchased from Allred Associates. The shutter blade is fastened to a hardened steel ring. The inner diameter of the ring has a vee profile, which rides on 6 ball-bearing guide wheels mounted to the shutter chassis. The outer diameter of the ring has a toothed profile which meshes with a Kevlar reinforced toothed drive belt. The belt is driven by a toothed pulley driven by a DC servo motor. An absolute rotary encoder is mounted at the center of the shutter blade. A flexural mount on the encoder body ensures concentricity between encoder axis and shutter axis. The timing and position control of the shutter is achieved using position, velocity, and time (PVT) trajectory interpolation. Minimum required exposure is 1 second which is easily achieved by ramping up to a constant velocity. Longer exposures typically have an open command and a close command with a pause between for the exposure time. Tests have verified 5 millisecond accuracy for the timing of the shutter over thousands of actuations. Lifetime testing has already logged the equivalent of several years of operations.

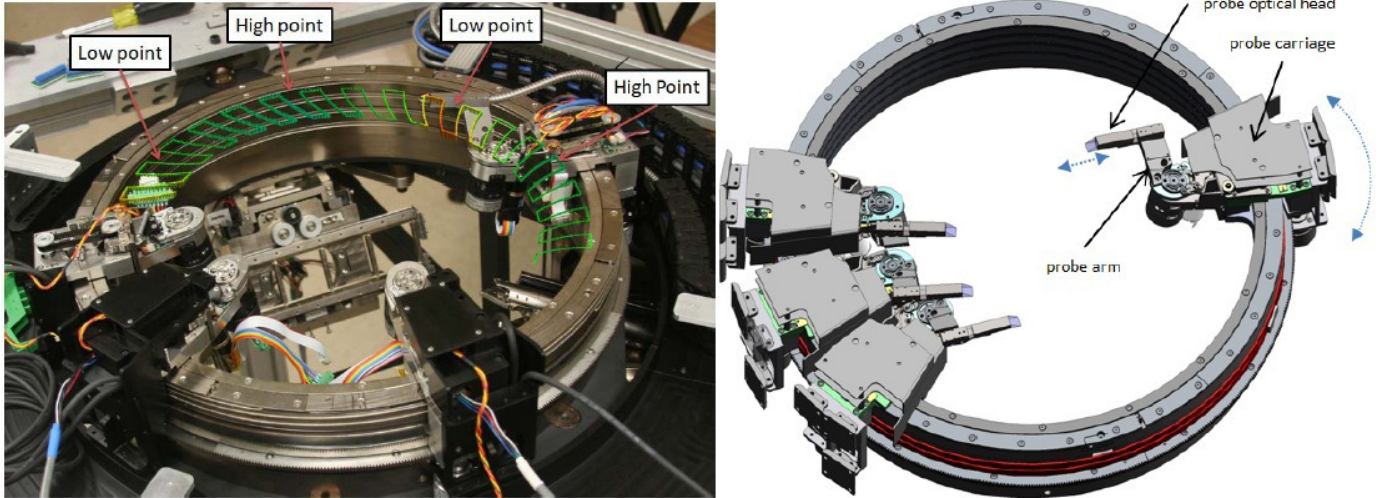


Figure 7. Guide probe assembly. Left shows the assembly undergoing performance tests with the LT. Peak to peak error is 30 microns, well within specification for focus. The layout and ability for the probes to nest very closely while avoiding any collision is shown on the right.

The dithering mechanism (Fig. 8) is a three position actuator that mounts the input head mount plate (IHMP) for the fiber feeds offsets fibers so that a set of three exposures will fill the interstitial space between fibers in a single VIRUS IFU<sup>32</sup>. The device is actuated by six Festo “fluidic muscle” pneumatic actuators; two are active in each of three positions. These actuators were selected for their high initial force and small diameter. They are particularly well suited for short-throw applications. A special pin flexure of titanium was designed to control the motion of the dithering mechanism. The design required a ~150 micron movement in a plane normal to the optical axis but only allowed for ~5 micron motion parallel to the optical axis despite the varying loads expected from the fiber feeds. Repeatability of motion has been demonstrated to be 5 microns rms, unloaded.

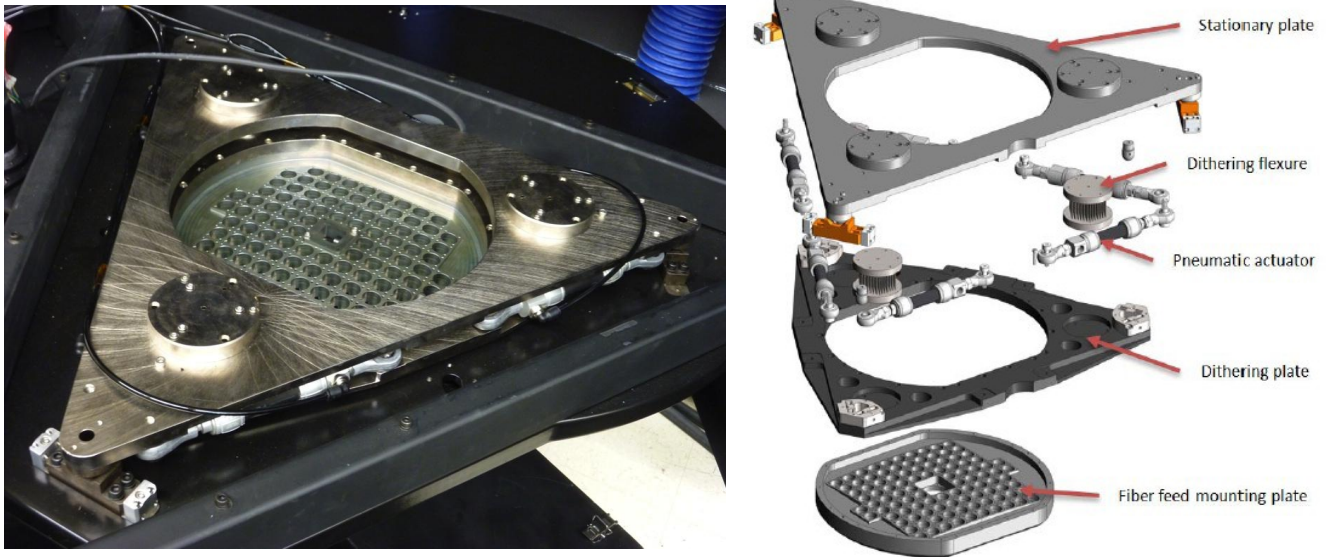


Figure 8. Dither mechanism that moves the VIRUS IFU heads between three precisely defined and repeatable positions. The exploded view on the right shows the components. The titanium flexures ensure that the assembly will carry the loads it will see during operation and still allow the small motions required. Left shows the assembled mechanism undergoing tests in the lab.

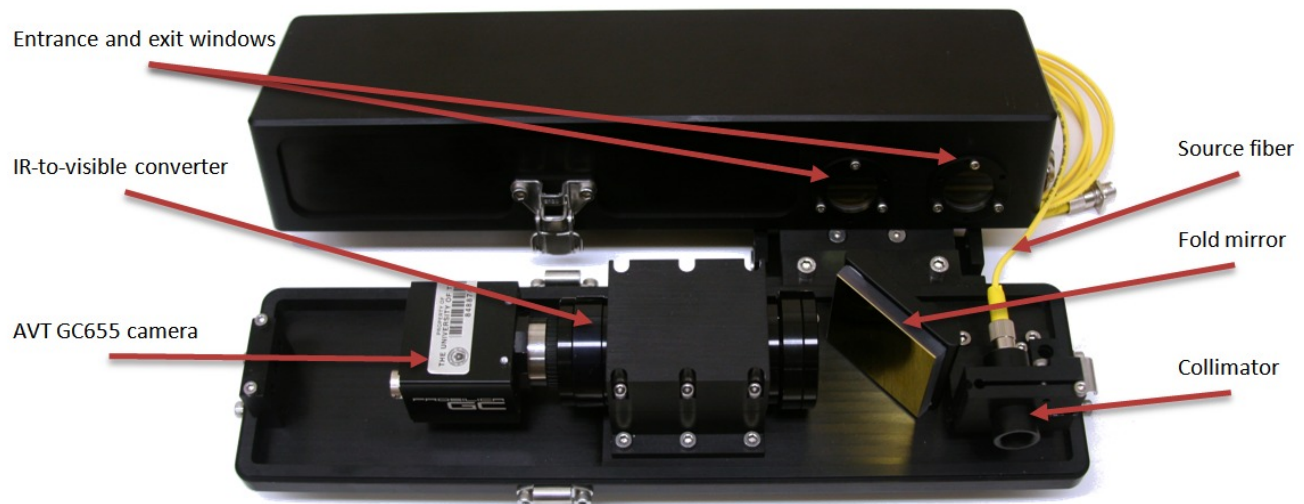


Figure 9: New Tip-Tilt Sensor (TTS) for the WFU. This metrology instrument monitors the angle between the WFC and the normal to the primary mirror as the HET tracks by projecting a 1.6 micron wavelength beam and measuring the position of the return reflection on a standard CCD camera via an IR to visible light converter reimaging lens system.

The LIP mounts to the WFC directly, and houses the entrance window selector and the facility calibration unit (FCU) input head. The FCU illuminates the pupil and focal surface of HET with a pattern almost indistinguishable from that obtained on sky<sup>33</sup>.

The PFIP has many precision mechanisms and is required to meet specifications over a temperature range of -5 to 25 Celsius, and operate down to -10 Celsius. In order to test the PFIP environmental specifications, we undertook an extensive program of cold-testing, including all mechanisms and cameras being constantly moved over a period of three days and nights. We utilized a rented refrigerated truck for these tests and took the PFIP and FCU through several temperature cycles over the test period<sup>18</sup>. The only issue that was uncovered was increased torque needed to actuate two of the GPs at temperatures below freezing, which led to motor current limits being reached and following errors. Investigations led us to remake two of the large bearing housings (Fig 7) which were slightly out of specification in roundness and to replace the grease in the bearings with a very light film of Dri-Slide lubricant. Further testing is scheduled, followed by realignment of the subassemblies of the FPA<sup>18</sup>.

## 6. METROLOGY SYSTEMS

HET requires constant monitoring and updating of the position of its components in order to deliver good images. The WFC must be positioned to 10  $\mu\text{m}$  precision in focus and X, Y, and 4.0 arcsec in tip/tilt with respect to the optical axis of the primary mirror. This axis changes constantly as the telescope tracks, following the sidereal motions of the stars. Tilts of the WFC cause comatic images. In addition, the global radius of curvature of the primary mirror can change with temperature (as it is essentially a glass veneer on a steel truss), and needs to be monitored. The segment alignment maintenance system (SAMS) maintains the positions of the 91 mirrors with respect to each other, but is less sensitive to the global radius of curvature of the surface. The feedback to maintain these alignments requires excellent metrology, which is provided by the following subsystems:

- Guide probes to monitor the position on the sky, and plate scale of the optical system, and monitor the image quality and atmospheric transparency
- Wavefront sensors (WFS) to monitor the focus and tilt of the WFC
- Distance measuring interferometer (DMI) to maintain the physical distance between the WFC and primary mirror
- Tip-tilt sensor (TTS) to monitor the tip/tilt of the WFC with respect to the optical axis of the primary mirror

The upgrade adds wavefront sensing<sup>19-22</sup> to HET in order to close the control loop on all axes of the system, in conjunction with the DMI adapted from the current tracker metrology system and a new TTS<sup>17</sup> (Fig. 9). There is redundancy built into the new metrology system in order to obtain the highest reliability. Two guide probes distributed

around the periphery of the field of view provide feedback on position, rotation, and plate scale, as well as providing a record of image quality and transparency as a function of wavelength. The alignment of the corrector is monitored by the wavefront sensors as well as by the DMI and TTS. The radius of curvature of the primary mirror is monitored by the combination of focus position from the WFS with the physical measurement from the DMI and checked by the plate scale measured from the positions of guide stars on the guide probes. The SAMS edge-sensors provide a less sensitive but redundant feedback on radius of curvature as well.

The two guide probes use small pick-off mirrors and coherent imaging fiber bundles to select guide stars from the outer annulus of the field of view. They are located ahead of the focal surface, before the shutter. Each ranges around the focal surface on precision encoded stages, accessing a 180 degree sector. They are designed to have a small size to reduce shadowing of the focal surface, and each has a field of view of 22.6 arcsec on a side. During setup on a new target, they will be driven to pre-defined positions, and the initial pointing will be made by centering the guide stars in the probes. This system is a significant upgrade from the former pellicle-based guiders on HET.

Two Shack-Hartmann (S-H) wavefront sensors also range in the outer field. Their function is to provide feedback on the low-order errors in the wavefront (focus, coma, spherical, and astigmatism)<sup>19-22</sup>. These errors are caused by misalignment of the corrector with the primary mirror focal surface and by global radius of curvature and astigmatism errors in the primary mirror shape. Updates will be generated approximately once per minute. In addition to the WFS probes there is an analysis wavefront sensor, selectable within the FPA by deploying a pickoff mirror, that will allow more detailed feedback analysis of the image quality, simultaneous with the operation of the WFS probes, independent of seeing. Simulations show that a S-H system with 7x7 sub-apertures across the pupil can meet the requirements using 18<sup>th</sup> magnitude stars. We have deployed a wavefront sensor for the current HET with 19 sub-apertures across the pupil and the final design is being informed by direct experience with this sensor. The design of the wavefront sensors is straightforward, but their application to the HET, with the varying illumination of the telescope pupil during a track, requires development of a robust software system for analysis of the sensor data to produce reliable wavefront information<sup>21</sup>.

With the delay in delivery of the WFC, we are proceeding to implement a subset of the metrology systems to support software development and mount-modeling. These include the TTS, DMI, and using a customized and automated video alignment telescope (VAT) for on-sky feedback. These three systems essentially replicate the feedback loops available on the HET before it was decommissioned.

## 7. SOFTWARE

The software effort is well into the implementation phase. It uses a component architecture providing a high degree of monitoring, automation, scriptability and scalability. It consists of a network of control systems, each of which models a sub-set of closely coupled hardware. The control systems (CS) communicate with each other using simple but flexible messaging scheme encoding commands to subsystems and events informing of state changes. Each system is responsible for specific functions based on type or proximity to hardware, and is designed to be run autonomously. For engineering purposes, each subsystem can also be scripted independently of others. The primary systems for the WFU and VIRUS are the Telescope CS (TCS), the Prime Focus Instrument Package CS (PFIP-CS), the Payload Alignment CS (PAS), the VIRUS Data Acquisition CS (VDAS), and the Tracker motion CS (TMCS), along with a centralized logging system. In addition to these control systems, GUI interfaces for the telescope operator and resident astronomer have been developed. The TCS is responsible for coordinating the operation of all other CS and knowledge of the high-level astronomy-related state is restricted to TCS. PFIP-CS controls the hardware on PFIP, while the PAS is responsible for gathering metrology from various alignment systems, including the guiders, WFS, TTS, and the DMI needed to close all tracker-motion related loops. The logger is failsafe, logging into local databases if the central log-server is down. These local databases are synchronized automatically with the central log server when it is available. In addition to log messages, logging can be configured to log any subset of events generated by the system, to obtain very detailed execution traces. This is done without interfering with the operation of the CS generating no additional overhead or changes in timing. The primary operating system is Red Hat Enterprise Linux 6.x, 64-bit. The software was developed with an agile process using the standard GNU toolchain, and widely available libraries. The TCS is ready and has been used to drive tracker TMCS with trajectories and moves as it is installed on the HET. The PAS camera chain works for both of our adopted camera product lines, and all algorithms of the metrology solver have been established. The software for VDAS has read out multiple CCDs and will be developed further as larger subsections of the VIRUS detector system

come on line. Overall, the software schedule tracks the availability of hardware, and will be ready for installation and commissioning in the second half of 2014.

### 8. VIRUS INFRASTRUCTURE

The VIRUS spectrograph units take up a large volume and require a distributed liquid nitrogen (LN) cooling system<sup>11</sup>. The infrastructure to support VIRUS is a significant undertaking and is being integrated with the deployment of the WFU. Since the wavelength coverage of VIRUS extends down to 350 nm, the average fiber length had to be minimized commensurate with keeping the mass of the instrument off the telescope structure and providing sufficient access to the primary mirror and tracker with the HET man-lifts and crane. Following extensive optimization and evaluation by HET staff, we settled on a configuration with VIRUS units housed in two large enclosures flanking the telescope structure and riding on a separate air-bearing system during rotation of the telescope in azimuth (Fig. 1).

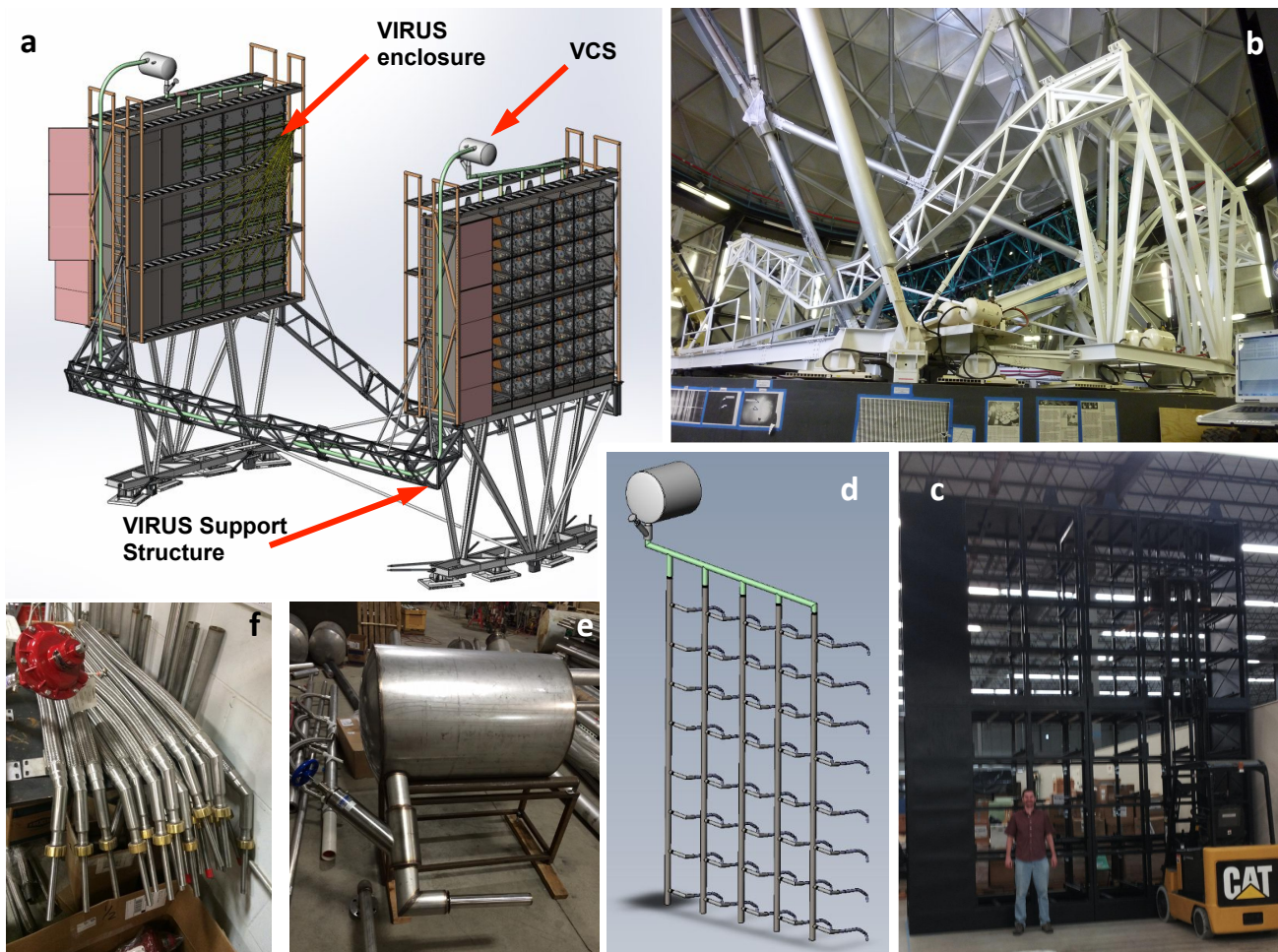


Figure 10: VIRUS infrastructure in development. From top left, clockwise (a) rendering of the VIRUS support structure (VSS), enclosures, and VIRUS cryogenic system (VCS), note the four air bearings at the base of each side, on which the structure lifts when the telescope changes azimuth; (b) the VSS installed, sitting on HET ringwall; (c) enclosure weldment for one side assembled at TAMU with a Québécois for scale; (d) schematic of the VCS for one enclosure, showing vertical sections each feeding 8 cameras and the phase separator tank; (e) and (f) show a phase separator and flex lines with bayonets that connect to individual VIRUS cameras at Midwest Cryogenics.

VIRUS units and the new LRS2 low-resolution spectrograph are housed in the large enclosures mounted on each side of the telescope. They are supported by the VIRUS support structure (VSS<sup>24</sup>) framework designed to carry the weight of the enclosures and spectrographs without connecting to the main structure of the telescope in order to ensure no coupling of wind-shake-induced motion into the tracking of the telescope. The VSS is shown in Fig. 10 both in rendering and as installed on the telescope. For changes in azimuth, the VSS rides on its own set of air bearings and is dragged by the main structure drives through loose linkages. When the structure is placed down, there is no significant coupling between the structures except through the concrete ring-wall pier at the base. The VSS was designed to withstand a catastrophic deceleration from full rotation speed without collapsing, though damage to the pier would be inevitable. We have not encountered any such incident in operating HET for 13 years.

The two large VIRUS enclosures are mounted to the VSS and are essentially sealed clean-rooms with a heat removal system to avoid degradation of the seeing by the heat generated by the detector controllers and electronics from escaping to the dome by convection or air leaks. They are based on large steel space-frames manufactured by SMK Manufacturing with skins and removable hatches to provide access to both sides of the spectrograph for camera maintenance and IFU access, respectively. The steel frames were analyzed with FEA to withstand the same impulses as the VSS. They have been procured by MDO and are being outfitted with hatches, seals, cables and the heat removal system by TAMU<sup>34</sup>. Tests of lightweight simple hatches that can be produced in quantity have shown excellent performance for air leakage rate.

The heat removal system is separate for each enclosure and uses ambient temperature facility glycol as the primary coolant fluid with a 600 W “Thermocube” thermoelectric cooler providing the ability to tune the temperature of the circulating air to keep the overall environment close to ambient temperature. It is needed to keep the VIRUS detector controllers from overheating and to remove the heat they generate so it does not enter the dome and degrade the seeing environment. Tests of prototype PVC ducting and custom attachment boot to the VIRUS controllers show excellent performance. Air is drawn through the controllers by the system and cold HEPA-filtered air is returned at the top of each sealed enclosure<sup>34</sup>. The enclosures will be delivered to HET between Sept and October so they are ready for VCS installation in November.



Figure 11. Google Earth view of the HET facility showing LN delivery truck maneuvering room at the telescope. The 11,000 gallon vacuum jacketed tank is located at the rear of the facility as indicated with fill tubes extending to the HET car park.

The distributed and large-scale layout of the VIRUS array presents a significant challenge for the cryogenic design<sup>11,35,36</sup>. Allowing 5 W heat load for each detector, with all losses accounted for and a 50% margin, the cooling

source is required to deliver 3,600W of cooling power. We engaged George Mulholand of Applied Cryogenics Technology to evaluate the options and provide an initial design. Following a trade-off between cryocoolers, small pulse-tubes and liquid nitrogen based systems, it is clear that from a reliability and cost point of view liquid nitrogen is the best choice<sup>35</sup>. The problem of distributing the coolant to the distributed suite of spectrographs is overcome with a gravity siphon system fed by a large external dewar. A trade-off between in-situ generation of the LN in an on-site liquefaction plant, and delivery by tanker has been made, with the result that the delivery option is both cheaper and more reliable. The 11,000 gallon vacuum jacketed holding dewar will be installed by Praxair in October 2014. It will have in excess of 4 weeks operation capacity and a 6,000 gallon delivery of LN will be required every two to three weeks. The delivery trucks are up to 65ft long and weigh as much as 80,000lb. After Praxair was awarded the LN supply contract we conducted a drive test with an empty delivery truck to confirm that roadway access to the telescope was adequate, and confirm that there is sufficient room to maneuver the delivery truck in the vicinity of the telescope building (Fig. 11).

An important aspect of the cryogenic design is the requirement to be able to remove a camera cryostat from the system for service, without impacting the other units. This is particularly difficult in a liquid distribution system. A design has been developed that combines a standard flexible stainless steel vacuum jacketed line (SuperFlex) to a cryogenic bayonet incorporating copper thermal connector contacts into each side of the bayonet. When the bayonet halves are brought together they close the thermal contact. The resulting system is completely closed, i.e., it is externally dry with no liquid nitrogen exposure. The camera end of the connector is connected by a copper cold finger to the detector. This design has another desirable feature: in normal operation the SuperFlex tube slopes downwards and the bayonet is oriented vertically. Liquid evaporation will flow monotonically up in order to avoid a vapor lock. If the bayonet is unscrewed and raised upwards, a vapor lock will occur and the bayonet will be cut off from the cooling capacity of the liquid nitrogen. This effectively acts as a “gravity switch”, which passively turns off cooling to that camera position.

We have made extensive tests on prototypes, applying heat loads to the bayonet, which have performed very well<sup>50</sup>. The temperature rise across the connection is  $\Delta T \sim 1.8$  K/Watt of load at 80 K. Modeling of the full thermal path has been undertaken, under the requirement of having the CCD temperature at -140 C, with no heater power. The performance of the bayonet is significantly better than the requirement, and represents less than 20 K temperature rise across the connection for the expected load. We will run the CCDs at about -110 C, controlled via heating resistors and a control loop based on an RTD sensor. The performance of the bayonet is not changed when the connection is broken and remade.

We have been running a lab cryogenic system for VIRUS testing for the past 4 years. It is a microcosm of the final VCS having a large external dewar, a header tank with “keep full” auto-fill system, and a single flex line and bayonet. The system is extremely reliable, and has been used to demonstrate that the VIRUS cryostats will hold vacuum, when kept cold, for at least 4 months without external intervention such as use of an ion pump. This performance allows us to avoid the cost of adding ion pumps and vacuum gauges to each camera, and instead rely on a maintenance regimen at HET that regularly warms, vacuum pumps, and then re-cools the cryostats in-situ, every 3-4 months. Based on the extensive prototype testing we are confident that the full cryogenic system will be robust. We have been using such systems in labs at VIRUS partner institutions for several years<sup>11</sup>, and find them very easy to use.

The contract for the fabrication of the VCS is awarded to Midwest Cryogenics. In the process of working with Midwest Cryogenics we discovered issues associated with the manufacturability and maintainability of our initial design<sup>35,36</sup> for the VCS components that reside in/on the VIRUS spectrograph enclosures. After working closely with Midwest Cryogenics a much-improved design emerged (Fig. 10(d)). The design is easier to fabricate and maintain, has lower heat loss, and is significantly less expensive. However, because the new design is very different than the initial design (that was recommended by our very seasoned cryogenic system expert George Mulholand) we felt it necessary to qualify the design by conducting a functional performance test.

Before proceeding with fabrication, a full-scale prototype of one of the vertical distribution pipes was fabricated and functionally tested at Midwest Cryogenics. The goal of the test was to verify that the pipe sizes would not compromise the two-phase flow thereby reducing the system’s ability to remove heat from the camera cryostats. The test setup is shown in Figure 12. The photograph on the right is a close-up view of some of test bayonets that were used to simulate the heat load imposed by VIRUS. Utilization of test bayonets in place of actual VIRUS camera cryostats greatly simplified the test logistics and reduced test cost. Each bayonet was equipped with an RTD (0.1°C resolution and  $\pm 0.2^\circ\text{C}$  accuracy) and a 20W heater. At the beginning of each test the bayonets were cooled with LN. After they reached thermal



equilibrium their temperature was monitored as various combinations of the bayonet heaters were turned on to simulate anticipated and extreme heat loads. Test bayonets were calibrated in our lab against an actual VIRUS camera cryostat prior to conducting tests at Midwest Cryogenics. During the calibration process we found that a test bayonet heater setting of 8.72W accurately mimics the heat load imposed by a VIRUS camera cryostat.



Figure 12. Functional performance test setup of VCS components at Midwest Cryogenics. Right is a close-up view of some of test bayonets that were used to simulate the heat load imposed by VIRUS. Left gives a sense of the scale of the system.

Test results indicated that the new VCS design meets our functional performance requirement. When we tried heating in extremis several bayonets to try and disrupt the cooling system we found the heating to not be disruptive, which is encouraging for the functioning of the fully populated vertical. We tried both heating seven as well as heating one at a time (for each bayonet) and found no problems. Note that the test bayonet heaters were set to 20W for these tests, so they were producing 2.3 times more heat than a VIRUS cryostat. The measured fluctuations of the unheated bayonet (when the other seven were set to 20W) was no more than about  $\pm 0.5^{\circ}\text{C}$ ; well within the requirement of  $\pm 1.5^{\circ}\text{C}$ .

An essential part of VCS is its safety system. This system continuously monitors critical variables (e.g. dome atmosphere oxygen levels, LN pressure, LN flow rates, and LN storage tank levels). When predefined set points are exceeded the system automatically activates strategically located audio and visual alarms, and if required closes the main LN supply line valve. The heart of the safety system is a Sensaphone SCADA 3000. It can handle up to 144 digital/analog I/O channels and can automatically place telephone calls (with prerecorded messages) to operations personnel. All data/control signals between the main electrical enclosure (which houses the SCADA 3000) and facility sensors/actuators are via fiber optic links (model AFL-80 and AFL-220 transmitter/receiver pairs) that are made by A. A. Labs System LTD in Israel. Safety system power is derived from a single UPS that is dedicated 100% to the safety system, and is backed up by the facility generator.

At the time of writing, the first phase of VCS installation is complete, running from the location of the external tank, through the azimuth wrap of the HET. The second phase will be executed after the enclosures are in place, since the VJ piping needs to be threaded into the enclosures. It will then be commissioned prior to installing spectrographs. The VCS is due to be installed by the end of November 2014.

## 9. INSTALLATION AND COMMISSIONING

Installation of the WFU and VIRUS has several phases. The first was removal of the old tracker and installation of the new tracker as described above, and installation and commissioning of the VSS. With the late delivery of the WFC, we are proceeding with important alignment and mount-modeling activities that retire risk once the WFC arrives. The tracker has WFC and PFIP test masses installed that mimic the payload closely and allow the performance of the tracker to be tuned and deflections modeled. This second phase has started and we have aligned the axis of the WFC test mass to the center segment of the primary mirror with the VAT and confirmed that the axis is aligned with the primary mirror center of curvature as defined by the source in the Mirror Alignment Recovery System (MARS<sup>37</sup>) in the center of curvature tower, which is used to stack the mirror segments to a common center of curvature at the start of each night. The TTS tilt sensor has been installed and aligned and the DMI will be mounted in early July when it returns from Fogle Nanotech where the working distance has been adjusted for the new WFC.

Mount modeling has commenced, using a LT to map deflections and tilts of the tracker payload over the full range of motion, and deflections of the telescope relative to the pier as the tracker moves. These measurements will allow the majority of the physical mount modeling to be completed before on-sky observations commence. This is a significant improvement on the methodology we had to adopt in commissioning the original HET where the highly convolved effects of flexure and the control system had to be deduced solely from on-sky measurements. We expect the mount-model for the WFU resulting from the direct LT measurements to be much better defined, to be better related to the physical effects being corrected, and to require significantly less time to implement and confirm.

The TCS software has successfully executed moves and tracks and is ready for first on-sky testing in July using the VAT, DMI and TTS to provide feedback loops on the movement of the tracker. This system will be used to commission a significant part of the control software and tools ahead of the delivery of the WFC so that we can go on-sky with the corrector as quickly as possible. Having this system in place for several months before the WFC arrives on-site will allow the system to be tested and refined and thereby speed final commissioning with the WFC.

In parallel with the WFU installation, the primary mirror segments are being recoated with a dense Aluminum reflective coating in a new coating facility on site. By the time of resumption of science operations mid 21015, all segments will have been cycled through the facility. Recoating and cleaning with dry ice snow will be an ongoing effort to maintain the primary mirror reflectivity in the best possible state. Reflectivity will be monitored with a 3-color CCD camera pupil viewer in the FPA. The other major activity while the WFU is being installed and commissioned is an upgrade to the thermal management of the facility. Heat removal to a remote dump is being integrated with VCS infrastructure.

## 10. SUMMARY

HET was taken off line at the end of August 2013. The removal of the old spherical aberration corrector, PFIP, and tracker followed by the installation of the new tracker was complete as of May 2014. We are now in the initial commissioning phase for the hardware and software while work continues at UA OSC to complete alignment of the WFC. If the WFC effort goes according to plan, we will take delivery at the end of 2014. On that schedule, instrument commissioning can start in Q2 2015 and science operations in Q3 2015. A large amount of risk is retired now and we will spend the rest of 2014 commissioning the tracker and other systems as far as possible, and installing the VIRUS infrastructure. VIRUS units will be installed from December 2014 to March 2015, and IFUs once the telescope achieves first light.

## ACKNOWLEDGEMENTS

HETDEX is run by the University of Texas at Austin McDonald Observatory and Department of Astronomy with participation from the Ludwig-Maximilians-Universität München, Max-Planck-Institut für Extraterrestrische-Physik (MPE), Leibniz-Institut für Astrophysik Potsdam (AIP), Texas A&M University (TAMU), Pennsylvania State University, Institut für Astrophysik Göttingen, University of Oxford and Max-Planck-Institut für Astrophysik (MPA). In addition to Institutional support, HETDEX is funded by the National Science Foundation (grant AST-0926815), the State of Texas, the US Air Force (AFRL FA9451-04-2-0355), by the Texas Norman Hackerman Advanced Research

Program under grants 003658-0005-2006 and 003658-0295-2007, and by generous support from private individuals and foundations.

We thank the following reviewers for their valuable input at various stages in the project:

- Science Requirements Review 6-26-07, Roland Bacon, Gary Bernstein, Gerry Gilmore, Rocky Kolb, Steve Rawlings
- Preliminary Design Review 4-10-08, Bruce Bigelow, Gary Chanan, Richard Kurz, Adrian Russell, Ray Sharples
- PFIP Integration and Alignment Review 7-26-11, Larry Ramsey, Bruce Bigelow, Steve Smee, Mike Smith
- Tracker Factory Acceptance Test Plan Review 3-8-11, Povilas Palunas, Jeffrey Kingsley, Dave Chaney
- Wide Field Upgrade Readiness Review, 7-16-13, Daniel Fabricant, Fred Hearty

We thank the staffs of McDonald Observatory, the Hobby-Eberly Telescope, and the Center for Electromechanics, University of Texas at Austin, the University of Arizona College of Optical Sciences, and Department of Physics and Astronomy, TAMU, for their contributions to the HET Wide Field Upgrade. Our particular thanks go to Darragh O'Donoghue and Buddy Martin who acted as external reviewers during diagnosis of the figure error issues on the WFC.

## REFERENCES

- [1] Booth, J.A., Wolf, M.J., Fowler, J.R., Adams, M.T., Good, J.M., Kelton, P.W. Barker, E.S., Palunas, P., Bash, F.N., Ramsey, L.W., Hill, G.J., MacQueen, P.J., Cornell, M.E., Robinson, E.L., "The Hobby-Eberly Telescope Completion Project", in *Large Ground-Based Telescopes*, Proc SPIE 4837, 919 (2003)
- [2] Booth, J.A., MacQueen, P.J., Good, J.G., Wesley, G.L., Segura, P.R., Palunas, P., Hill, G.J., R.E. Calder, R.E., "The Wide Field Upgrade for the Hobby-Eberly Telescope", Proc. SPIE, 6267-97 (2006)
- [3] G.J. Hill, P.J. MacQueen, M.D. Shetrone, & J.A. Booth, "Present and future instrumentation for the Hobby-Eberly Telescope", Proc. SPIE, 6269-5 (2006)
- [4] Hill, G.J., MacQueen, P.J., Palunas, P., Barnes, S.I., Shetrone, M.D., "Present and future instrumentation for the Hobby-Eberly Telescope", Proc. SPIE, 7014-5 (2008)
- [5] Savage, R.D., Booth, J.A., Gebhardt, K., Good, J.M., Hill, G.J., MacQueen, P.J., Rafal, M.D., Smith, M.P., Vattiat, B.L., "Current Status of the Hobby-Eberly Telescope Wide Field Upgrade and VIRUS", *Proc. SPIE*, 7012-10 (2008)
- [6] Savage, R., et al., "Current Status of the Hobby-Eberly Telescope wide field upgrade," *Proc. SPIE*, 7733-149 (2010)
- [7] Buckley, D.A.H., Swart, G.P., Meiring, J.G., "Completion of the Southern African Large Telescope", *Proc. SPIE*, 6267-19 (2006)
- [8] Hill, G.J., MacQueen, P.J., Palunas, P., Kelz, A., Roth, M.M., Gebhardt, K., Grupp, F., "VIRUS: a hugely replicated integral field spectrograph for HETDEX", *New Astronomy Reviews*, 50, 378 (2006)
- [9] Hill, G.J., MacQueen, P.J., Smith, M.P., Tufts, J.R., Roth, M.M., Kelz, A., Adams, J.J., Drory, N., Barnes, S.I., Blanc, G.A., Murphy, J.D., Gebhardt, K., Altmann, W., Wesley, G.L., Segura, P.R., Good, J.M., Booth, J.A., Bauer, S.-M., Goertz, J.A., Edmonston, R.D., Wilkinson, C.P., "Design, construction, and performance of VIRUS-P: the prototype of a highly replicated integral-field spectrograph for HET", *Proc. SPIE*, 7014-257 (2008)
- [10] Hill, G.J., et al., "VIRUS: production of a massively replicated 33k fiber integral field spectrograph for the upgraded Hobby-Eberly Telescope," *Proc. SPIE*, 8446-21 (2012)
- [11] Hill, G.J., Tuttle, S.E., Drory, N., Lee, H., Vattiat, B.L., DePoy, D.L., Marshall, J.L., Kelz, A., Haynes, D., Fabricius, M., Gebhardt, K., Allen, R.D., Blanc, G., Chonis, T.S., Cornell, M.E., Dalton, G., Good, J., Jahn, T., Kriel, H., Landriau, M., MacQueen, P.J., Murphy, J.D., Prochaska, T., Nicklas, H., Ramsey, J., Roth, M.M., Savage, R., Snigula, J., "VIRUS: production and deployment of a massively replicated fiber integral field spectrograph for the upgraded Hobby-Eberly Telescope", Proc. SPIE, 9147-25 (2014)
- [12] Hill, G.J., Gebhardt, K., Komatsu, E., Drory, N., MacQueen, P.J., Adams, J.A., Blanc, G.A., Koehler, R., Rafal, Roth, M.M., Kelz, A., Grupp, F., Murphy, J., Palunas, P., Gronwall, C., Ciardullo, R., Bender, R., Hopp, U., and Schneider, D.P., "The Hobby-Eberly Telescope Dark Energy Experiment (HETDEX): Description and Early Pilot Survey Results", in *Panoramic Views of the Universe*, ASP Conf. Series, 399, 115 (2008)
- [13] Burge, J.H., Benjamin, S.D., Dubin, M.B., Manuel, S.M., Novak, M.J. Oh, C.J., Valente, M.J., Zhao, C., Booth, J.A., Good, J.M., Hill, G.J., Lee, H., MacQueen, P.J., Rafal, M.D., Savage, R.D., Smith, M.P., Vattiat, B.L.,

- “Development of a wide-field spherical aberration corrector for the Hobby Eberly Telescope”, Proc. SPIE, 7733-51 (2010)
- [14] Oh, C.-J., Frater, E., Zhao, C., Burge, J.H., “System alignment and performance test of a wide field corrector for the Hobby-Eberly telescope”, Proc. SPIE, 9145-8 (2014)
- [15] Good, J., et al., “Design of performance verification testing for HET wide-field upgrade tracker in the laboratory,” Proc. SPIE, 7739-152 (2010)
- [16] Good, J.M., Hill, G.J., Leck, R.L., Landriau, M., Drory, N., Fowler, J.R., Kriel, H., Cornell, M.E., Booth, J.A., Lee, H., Savage, R., “Laboratory Performance Testing, Installation, and Commissioning of the Wide Field Upgrade Tracker for the Hobby-Eberly Telescope”, Proc. SPIE, 9145-156 (2014)
- [17] Vattiat, B.L., et al., “Design, testing, and performance of the Hobby Eberly Telescope prime focus instrument package,” Proc. SPIE, 8446-269 (2012)
- [18] Vattiat, B.L., Hill, G.J., Lee, H., Moreira, W., Drory, N., Ramsey, J., Elliot, L., Landriau, M., Perry, D.M., Savage, R., Kriel, H., Haeuser, M., Mangold, F., “Design, alignment, and deployment of the Hobby Eberly Telescope prime focus instrument package”, Proc. SPIE, 9147-172 (2014)
- [19] Lee, H., et al., “Analysis of active alignment control of the Hobby-Eberly Telescope wide field corrector using Shack-Hartmann wavefront sensors,” Proc. SPIE, 7738-18 (2010)
- [20] Lee, H., et al., “Metrology systems for the active alignment control of the Hobby-Eberly Telescope wide-field upgrade,” Proc. SPIE, 7739-28 (2010)
- [21] Lee, H., et al., “Orthonormal aberration polynomials over arbitrarily obscured pupil geometries for wavefront sensing in the Hobby-Eberly Telescope,” Proc. SPIE, 7738-59 (2010)
- [22] Lee, H., et al., “Metrology systems of Hobby-Eberly Telescope wide field upgrade,” Proc. SPIE, 8444-181 (2012)
- [23] Lee, H., et al., “Surface figure measurement of the Hobby-Eberly Telescope primary mirror segments via phase retrieval and its implications for the wavefront sensing in the new wide-field upgrade,” Proc. SPIE, 7738-58 (2010)
- [24] Worthington M., et al., “Design of VIRUS spectrograph support structure for the Hobby-Eberly Telescope dark energy experiment (HETDEX),” Proc. SPIE, 8444-213 (2012)
- [25] Mollison, N.T., et al., “Design and development of a long-travel positioning actuator and tandem constant force actuator safety system for the Hobby-Eberly Telescope wide field upgrade,” Proc. SPIE, 7733-150 (2010)
- [26] Zierer, Jr., J.J., Wedeking, G.A., Beno, J.H., Good, J.M., “Design, testing, and installation of a high-precision hexapod for the Hobby-Eberly Telescope dark energy experiment (HETDEX),” Proc. SPIE, 8444-176 (2012)
- [27] Worthington, M.S., et al., “Design and development of a high-precision, high-payload telescope dual-drive system,” Proc. SPIE, 7733-201 (2010)
- [28] Soukup I.M., et al., “Testing, characterization, and control of a multi-axis, high precision drive system for the Hobby-Eberly Telescope Wide Field Upgrade,” Proc. SPIE, 8444-147 (2012)
- [29] Hayes, R.H., et al., “Use of failure modes and effects analysis in design of the tracker system for the HET wide-field upgrade,” Proc. SPIE, 8449-56 (2012)
- [30] Beno, J.H., *et al.*, “HETDEX tracker control system design and implementation,” Proc. SPIE, **8444**-211 (2012)
- [31] Good, J.M., Lee, H., Hill, G.J., Vattiat, B.L., Perry, D., Kriel, H., Savage, R., “Design and Implementation of Coating Hardware for the Hobby-Eberly Telescope Wide Field Corrector”, Proc. SPIE, 9145-160 (2014)
- [32] Kelz, A., Jahn, T., Haynes, D.M., Hill, G.J., Murphy, J.D., Rutowska, M., Streicher, O., Neumann, J., Nicklas, N., Sandin, C., Fabricius, M., “HETDEX / VIRUS: testing and performance of 33,000 optical fibres”, Proc. SPIE, 9147-269 (2014)
- [33] Lee, H., Hill, G.J., Vattiat, B.L., Smith, M.P., Haeuser, M., “Facility calibration unit of Hobby Eberly Telescope wide field upgrade,” Proc. SPIE, 8444-172 (2012)
- [34] Prochaska, T., Allen, R., Rheault, J. P., Cook, E., Baker, D., DePoy, D. L., Marshall, J. L., Hill, G., Perry, D., “VIRUS instrument enclosures,” Proc. SPIE 9147-257 (2014)
- [35] Smith, M.P., Mulholland, G.T., Booth, J.A., Good, J.M., Hill, G.J., MacQueen, P.J., Rafal, M.D., Savage, R.D., Vattiat, B.L., “The cryogenic system for the VIRUS array of spectrographs on the Hobby Eberly Telescope”, Proc. SPIE, 7018-117 (2008)
- [36] Chonis, T.S., et al., “Development of a cryogenic system for the VIRUS array of 150 spectrographs for the Hobby-Eberly Telescope,” Proc. SPIE, 7735-265 (2010)
- [37] Wolf, M.J., Ward, M., Booth, J.A., Wirth, A., Wesley, G.L., O’Donoghue, D., & Ramsey, L.W., “Mirror Alignment Recovery System on the Hobby-Eberly Telescope”, Proc SPIE 4837, 714 (2003)